The twistor discriminant locus of the Fermat cubic

John Armstrong

ABSTRACT. We consider the discriminant locus of the Fermat cubic under the twistor fibration $\mathbb{CP}^3 \longrightarrow S^4$. We show that it has a conformal symmetry group of order 72. Using these symmetries we reduce the problem of computing the topology of this discriminant locus to a computationally feasible problem which we solve using the cylindrical algebraic decomposition algorithm.

CONTENTS

1. Introduction

Orientation preserving conformal maps of $S^4 = \mathbb{R}^4 \cup \{\infty\}$ to itself give rise, via the twistor construction, to projective transformations of the twistor space $\mathbb{CP}^3$. So, in the spirit of Klein's Erlangen program, one can choose to consider the classical geometry of $\mathbb{CP}^3$ modulo the projective transformations or the twistor geometry of $\mathbb{CP}^3$ modulo the orientation preserving conformal maps of S^4. In particular instead of classifying algebraic surfaces up to projective transformation, one can instead attempt to classify them up to orientation preserving conformal transformation.

For the sake of brevity, in the rest of this paper, we will redefine conformal to mean orientation and angle preserving rather than merely angle preserving.

The defining polynomial equation of a degree d complex surface Σ in $\mathbb{CP}^3$ reduces to a polynomial in one variable of degree d on each fibre of the twistor fibration. So when restricted to Σ, the twistor fibration gives a d-sheeted cover S^4. The branch locus is given by the points where the discriminant of the polynomial on each fibre vanishes, hence this is called the discriminant locus.

The topology of the discriminant locus is an invariant of Σ under the conformal group. Thus understanding the topology of the discriminant locus is a natural question when classifying surfaces modulo the conformal group.

Related to the study of the discriminant locus is the study of twistor lines. If a fibre of the twistor projection is contained in Σ, then the polynomial on that fibre completely vanishes. Such a fibre is called a twistor line of Σ. Its projection onto S^4 is a singular point of the discriminant locus.

The classification of nonsingular degree 2 surfaces under conformal transformations was completed in [12]. The classification shows that for nonsingular degree 2 surfaces there are always either 0, 1, 2 or ∞ fibres of the twistor fibration lying on the surface and that the topology of the discriminant locus is completely determined by the number of twistor lines.

A study of twistor lines on cubic surfaces was made in [1]. The aim of this paper is to consider the topology of the discriminant locus on such surfaces and, in particular, to calculate the topology of the discriminant locus for the Fermat cubic. This is the cubic surface given by the equation

$$(1.1) \qquad\qquad z_1^3 + z_2^3 + z_3^3 + z_4^3 = 0.$$

A key ingredient in the proof is the observation that the discriminant locus has a surprisingly large conformal symmetry group of order 72. By contrast, the Fermat cubic itself has only 6 conformal symmetries.

The question of computing the topology of the discriminant locus in degrees $d \geq 2$ was raised in [11]. The topology of a projectively, but not conformally, equivalent cubic surface was computed informally in [2]. However, the argument in [2] is not fully rigorous since it depends upon visual examination of the discriminant locus. This paper contains the first fully rigorous calculation of the discriminant locus of an irreducible surface of degree $d \geq 2$.

The structure of the remainder of the paper is as follows.

We begin by clarifying our notation and reviewing the twistor fibration in Section 2. The reader should consult [3] for further background on the Twistor fibration.

In Section 3 we prove the basic algebraic facts about the discriminant locus. We show in particular how to choose coordinates that significantly

reduce the algebraic complexity of the discriminant locus when it has a twistor line.

In Section 4 we prove some general facts about the topology of the discriminant locus. In particular we compute its Euler characteristic, dimension and orientability and consider its (non)-smoothness properties.

In Section 5 we review the classification of surfaces with isolated singularities. The purpose of this is to establish a graphical notation which we can use to unambiguously describe the topology of a singular surface.

In Section 6 we compute the topology of the discriminant locus of the Fermat cubic using a visual inspection. The aim of the remaining two sections is to provide a rigorous justification for this computation. In Section 7 we analyse the symmetries of the discriminant locus which allows us to significantly simplify the problem. With these simplifications in place, in Section 8 we are able to apply the cylindrical algebraic decomposition algorithm to complete the proof.

2. Review of the twistor projection $\mathbb{CP}^3 \to S^4$

Let us quickly review the setup.

Define two equivalence relations on $(\mathbb{H} \times \mathbb{H}) \setminus \{0\}$, denoted $\sim_\mathbb{C}$ and $\sim_\mathbb{H}$, by

$$(q_1, q_2) \sim_\mathbb{H} (\lambda q_1, \lambda q_2) \quad \lambda \in \mathbb{H} \setminus \{0\}$$
$$(q_1, q_2) \sim_\mathbb{C} (\lambda q_1, \lambda q_2) \quad \lambda \in \mathbb{C} \setminus \{0\}$$

$((\mathbb{H} \times \mathbb{H}) \setminus \{0\}) / \sim_\mathbb{C} \cong \mathbb{CP}^3$ and $((\mathbb{H} \times \mathbb{H}) \setminus \{0\}) / \sim_\mathbb{H} \cong \mathbb{H}P^1 \cong \mathbb{R}^4 \cup \{\infty\} \cong S^4$. An explicit map from $\mathbb{CP}^3$ to $((\mathbb{H} \times \mathbb{H}) \setminus \{0\}) / \sim_\mathbb{C}$ is given by

$$[z_1, z_2, z_3, z_4] \to [z_1 + z_2 j, z_3 + z_4 j]_{\sim_\mathbb{C}}.$$

The map $\pi : [q_1, q_2]_{\sim_\mathbb{C}} \longrightarrow [q_1, q_2]_{\sim_\mathbb{H}}$ is the twistor fibration.

Left multiplication by the quaternion j induces an antiholomorphic involution of $\mathbb{CP}^3$ given by $[q_1, q_2]_{\sim_\mathbb{C}} \mapsto [jq_1, jq_2]_{\sim_\mathbb{C}}$. We will call this involution j, it should be clear from the context whether we are referring to the quaternion j or to this map. The map j acts on each fibre of π as the antipodal map.

The group of conformal transformations of S^4 is given by the quaternionic Möbius transformations acting on the quaternionic projective space on the right. That is for 4 quaternions a, b, c, d we define the associated Möbius transformation by:

$$[q_1.q_2]_\sim \to [q_1 a + q_2 b, q_1 c + q_2 d]_\sim.$$

This can be viewed either as a conformal transformation of S^4 or as a fibre preserving holomorphic map of $\mathbb{CP}^3$. Thinking of S^4 as $\mathbb{H} \cup \{\infty\}$ we can write this map as:

$$q \to (qc + d)^{-1}(qa + b).$$

If we use the notation $q = q_1 + q_2 j$ to split a quaternion into two complex components q_1 and q_2 then we can explicitly write the projective transformation associated with the Möbius transformation $(qc + d)^{-1}(qa + b)$ as:

$$\begin{pmatrix} a_1 & -\overline{a_2} & b_1 & -\overline{b_2} \\ a_2 & \overline{a_1} & b_2 & \overline{b_1} \\ c_1 & -\overline{c_2} & d_1 & -\overline{d_2} \\ c_2 & \overline{c_1} & d_2 & \overline{d_1} \end{pmatrix}.$$

Thus a projective transformation arises from a conformal transformation of S^4 if and only if it has the complex conjugation symmetries shown in the matrix above.

Let us give formal definitions of the central notions in this paper:

Definition 2.1. The *discriminant locus* $\mathcal{D}$ of a degree d complex surface Σ in $\mathbb{CP}^3$ is the set:

$$\{x \in S^4 : \#(\pi^{-1}(x) \cap X) \neq d\}.$$

Definition 2.2. A *twistor line* of Σ is a fibre of π which lies entirely within Σ.

Definition 2.3. When $d = 3$ we define the set of *triple points* of Σ to be the set:

$$\{x \in S^4 : \#(\pi^{-1}(x) \cap X) = 1\}.$$

3. Algebraic properties of the discriminant locus

We can now state the main algebraic results about the discriminant locus.

Proposition 3.1. *With the exception of a possible point at ∞, the discriminant locus of a general degree d surface is described by the zero set of a complex valued polynomial of degree $2d(d-1)$ in the real coordinates $\mathbf{x} = (x_1, x_2, x_3, x_4)$ for $S^4 = \mathbb{R}^4 \cup \{\infty\}$. If the surface contains a twistor line over ∞ this simplifies to a polynomial of degree $2(d-1)^2$.*

Proof. Let the surface be defined by the equation $f(z_1, z_2, z_3, z_4) = 0$ for a homogeneous polynomial f of degree d.

Define a map $p_1 : \mathbb{R}^4 \longrightarrow \mathbb{H}$ by $p_1(x_1, x_2, x_3, x_4) = x_1 + x_2 i + x_3 j + x_4 k$. Define $p_2 = j \circ p_1$.

Define $\psi : \mathbb{R}^4 \times \mathbb{CP}^1 \longrightarrow \mathbb{CP}^3$ by $\psi(\mathbf{x}, [\lambda_1, \lambda_2]) = [\lambda_1 p_1(\mathbf{x}) + \lambda_2 p_2(\mathbf{x})]$. Thinking of S^4 as $\mathbb{R}^4 \cup \{\infty\}$, one sees that ψ gives a trivialization of the twistor fibration away from the point ∞.

Viewing $\mathbb{R}^4$ as $\mathbb{C} \times \mathbb{C}$ we can define $p_1(w_1, w_2)$ for complex numbers $w_1 = x_1 + ix_2$ and $w_2 = x_3 + ix_4$. So $f \circ p_1$ is an inhomogeneous polynomial in w_1, w_2 of degree at most d. Its zero set defines a complex affine curve $\mathcal{C}_1$. This affine curve is mapped by p_1 to the intersection of the surface $f = 0$ and the affine plane in $\mathbb{CP}^3$ defined by the conditions $z_4 = 0$ and $z_3 \neq 0$. $p_1(\mathcal{C}_1)$ thus lies inside the degree d curve $\mathcal{C}_2$ defined by the intersection of $f = 0$ and the plane $z_4 = 0$.

If $\mathcal{C}_2$ is irreducible, we may conclude that $f \circ p_1$ is of degree exactly d. However if $\mathcal{C}_2$ contains the line defined by the conditions $z_3 = z_4 = 0$ then $f \circ p_1$ will be of degree at most $d-1$. We deduce that $f \circ p_1$ will be of degree less than d if the surface $f = 0$ contains the line $z_3 = z_4 = 0$. Equivalently $f \circ p_1$ will be of degree $\leq d-1$ if and only if the surface $f = 0$ contains the twistor line over ∞.

Using the same argument with a different identification of $\mathbb{R}^4$ and $\mathbb{C} \times \mathbb{C}$ gives the same result for $f \circ p_2$. Indeed one has this result for any function $f \circ (\lambda_1 p_1 + \lambda_2 p_2)$ for complex numbers $\{\lambda_1, \lambda_2\} \in \mathbb{C}^2 \setminus \{0\}$.

We deduce that the function $f(\mathbf{x}, \lambda) = f(p_1(\mathbf{x}) + \lambda p_2(\mathbf{x}))$ is a degree d polynomial in λ with coefficients of degree d in $\mathbf{x}$ (of degree less than d if $f = 0$ contains the twistor line over ∞). To see this write $f(\mathbf{x}, \lambda) = a_d(\mathbf{x})\lambda^d + a_{d-1}(\mathbf{x})\lambda^{d-1} + \ldots a_1(\mathbf{x})\lambda + a_0(\mathbf{x})$, for some polynomials a_i. Inserting the values $\lambda = 0, 1, 2, \ldots, d$ in this expression gives $d+1$ linearly independent expressions in the a_i in terms of the degree d (or $d-1$) polynomials $f(\mathbf{x}, \omega)$. Solving these equations allows us to express a_i as degree d (or $d-1$) polynomials.

Recall that the discriminant of a polynomial of degree d is a polynomial of degree $2(d-1)$ in the coefficients. The result now follows. $\square$

For cubic surfaces, the discriminant locus is of degree 12 or, if there is a twistor line, of degree 8.

We will also be interested in the number of triple points of a cubic surface. If we recall that the cubic $a\omega^3 + b\omega^2 + c\omega + d$ has a triple root if and only if $b^2 - 3ac = 0$ and $9ad - bc = 0$ we find from the argument above:

Proposition 3.2. *The set of triple points of a cubic surface is the zero set of two complex polynomials of degree* 6 *in* $\mathbf{x}$. *If there is a twistor line at* ∞ *these simplify to polynomials of degree* 4.

We make some remarks.

(i) The discriminant locus is defined by the zero set of a complex valued polynomial. Taking real and imaginary parts of this polynomial, the discriminant locus can be defined by intersection of the zero sets of two real valued polynomials.

(ii) It is straightforward to perform this calculation explicitly with a computer algebra system to find the explicit polynomials. When one notices that a general degree 12 polynomial in 4 variables has 1820 coefficients and a general degree 8 polynomial in 4 variables has 495 coefficients then the need for computer algebra in calculations becomes obvious.

(iii) The drop in the degree when one has a twistor line at infinity should be seen as a substantial simplification. Many of the known algorithms in computational geometry have computational complexity of the approximate form $p(d)^{c^{n-1}}$ where p is a polynomial in the degree d of the polynomials under consideration, n is the dimension and c is some

constant. Key examples of such algorithms are the computation of Gröbner bases (see [9, 6]) and of cylindrical algebraic decompositions (see [4]).

4. The topology of the discriminant locus

Let us make some general observations about the topology of the discriminant locus.

Definition 4.1. The *double locus* of $\mathcal{D}$ denoted $\mathcal{D}'$ is the set of points x in $\mathcal{D}$ where $f_{\restriction \pi^{-1}(x)}$ has a unique double point.

Proposition 4.2. *The discriminant locus $\mathcal{D}$ of a degree d complex surface Σ defined by the equation $f = 0$, with f a square free polynomial, is compact and of real dimension ≤ 2. The set $\mathcal{D}'$ is a smooth orientable real surface.*

Proof. The discriminant locus can locally be written as the zero set of a complex valued polynomial in the coordinates $\mathbf{x}$. Therefore it is compact.

Write $\Sigma = \Sigma^1 \cup \Sigma^2$ where Σ^1 consists of the smooth points of Σ and Σ^2 contains the nonsmooth points. Since f is square free, Σ^2 has complex dimension of one or less.

A point x_0 lies in $\mathcal{D} \backslash \pi(\Sigma^2)$ if and only if at some point $z \in \pi^{-1}(x) \cap \Sigma^1$, the tangent space $T_z\Sigma$ contains the tangent of the twistor fibre at z. Therefore the restriction of π to Σ^1 has rank 2 at z. The Sard–Federer theorem then implies that the Hausdorff dimension of $\mathcal{D} \setminus \pi(\Sigma^2)$ is ≤ 2. Since we are working in the real algebraic category, Hausdorff dimension and dimension coincide. So the real dimension of $\mathcal{D}$ is ≤ 2.

Suppose that x_0 is a point in $\mathcal{D}'$. Let z be the unique double point of $f_{\restriction \pi^{-1}(x_0)}$. As described in the proof of Proposition 3.1, we have a chart $\psi : \mathbb{R}^4 \times \mathbb{C}^2 \to \mathbb{CP}^3$ given by $\psi(\mathbf{x}, \lambda) \to [p_1(\mathbf{x}) + \lambda p_2(\mathbf{x})]$. We assume this chart is centred on z. Suppose that Σ is defined by the polynomial f and consider the function $F(\mathbf{x}, \lambda) = f \circ \psi$. F is holomorphic in the λ component and smooth in the $\mathbf{x}$ component. Since z lies in $\mathcal{D}'$ we have that F and $\frac{\partial F}{\partial \lambda}$ vanish at 0 but that $\frac{\partial^2 F}{\partial \lambda^2}$ does not. Define the map $g : \mathbb{R}^4 \times \mathbb{C} \to \mathbb{C}$ by $g = \frac{\partial F}{\partial \lambda}$. Σ is tangent to the fibre at z. $g_*(\frac{\partial}{\partial \lambda}) \neq 0$. Therefore when restricted to $T_z\Sigma$, the differential g_* has real rank 2. Note that the fact F is holomorphic in λ is the crucial point here. By the implicit function theorem $g^{-1}(0) \cap \Sigma$ is locally a smooth 2-manifold in a neighbourhood of z. Since $x_0 \in \mathcal{D}'$, π is a homeomorphism of a neighbourhood of z onto a neighbourhood of x_0. Thus $\mathcal{D}'$ is a smooth 2-manifold.

At z the tangent space $T_z\Sigma$ can be written as the sum of a vertical subspace V, given by the tangent space of the fibre and a horizontal subspace H with π_* mapping H isomorphically to the tangent space of the discriminant locus. There is a canonical symplectic form ω_V on V given by the pull-back of the Fubini–Study metric onto the fibre. Similarly there is a canonical symplectic form ω_Σ on $T_z\Sigma$. So we can say that a nondegenerate two form

ω_H is positively oriented if $\omega_V \wedge \omega_H$ is a positive multiple of ω_Σ. This defines an orientation of H and hence an orientation $T_{x_0}\mathcal{D}'$. $\square$

It is quite possible that the dimension of the discriminant locus of a surface Σ is strictly less than 2. For example: the discriminant locus of a plane is just a point; there exist quadrics whose discriminant locus is just a circle ([12]). The discriminant locus of a reducible surface is given by the union of the discriminant loci of the intersections and the image of the intersection of components under π. This allows one to manufacture singular surfaces with pathological discriminant loci. For example consider the cubic surface consisting of three planes intersecting in a line. If the line of intersection is a twistor line, the discriminant locus is a single point. If the line of intersection is not a twistor line, then the discriminant locus is a round sphere and all points in the discriminant locus are triple points or twistor lines.

Proposition 4.3. *If Σ is a nonsingular complex surface of degree d with $d > 2$ then its discriminant locus has dimension 2.*

Proof. We have already shown that the dimension of the discriminant locus is no greater than 2, so suppose for a contradiction that the discriminant locus $\mathcal{D}$ is 1 (or less) dimensional. Then $S^4 \setminus \mathcal{D}$ is simply connected. The restriction $\pi_{\restriction \Sigma \setminus (\pi^{-1}\mathcal{D})}$ is a d-sheeted cover of $S^4 \setminus \mathcal{D}$ with no branch points. Therefore $\Sigma \setminus (\pi^{-1}\mathcal{D})$ has d connected components. In particular it is disconnected if $d \geq 2$.

If Σ is nonsingular and $d > 2$ then Σ only contains a finite number of projective lines (see [5] for a survey of the known bounds). Given a point $x \in S^4$ then $\pi^{-1}(x)$ is either finite or a projective line. So $\pi^{-1}\mathcal{D}$ has dimension at most 2. Nonsingular complex surfaces are always connected. So $\Sigma \setminus (\pi^{-1}\mathcal{D})$ is connected.

This is the desired contradiction. $\square$

We next compute the Euler characteristic:

Proposition 4.4. *Let Σ be a nonsingular cubic curve. Let T denote the set of triple points of the twistor fibration and $\mathcal{D}$ be the discriminant locus. We have*:
$$\chi(\mathcal{D}) = -3 - \chi(T).$$

Proof. Let n denote the number of twistor lines. $\pi_{\restriction \Sigma}$ is a 3 sheeted cover of S^4 branched over the discriminant locus. There are two points in Σ over each point in $\mathcal{D}'$, 1 point over each triple point and a copy of $\mathbb{CP}^1$ for each twistor line. Hence by the additivity of the Euler characteristic:
$$\chi(\Sigma) = 3\chi(S^4 \setminus \mathcal{D}) + 2\chi(\mathcal{D}') + \chi(T) + n\chi(\mathbb{CP}^1).$$

All nonsingular cubics are diffeomorphic to $\mathbb{CP}^2 \# 6\overline{\mathbb{CP}^2}$. So $\chi(\Sigma) = 9$.
$$9 = 6 - 3\chi(\mathcal{D}) + 2(\chi(\mathcal{D}) - \chi(T) - n) + \chi(T) + 2n.$$

The result follows.   □

Corollary 4.5. *The set $\mathcal{D} \setminus \mathcal{D}'$ on a smooth nonsingular surface Σ of degree d is always nonempty if d is odd.*

Proof. Suppose that d is odd and that the twistor fibration contains no triple points or twistor lines. The discriminant locus will then be smooth, compact and orientable. So its Euler characteristic must be even.

The Euler characteristic of S^4 is even. Hence the Euler characteristic of a d fold cover of S^4 branched along the discriminant locus must also be even. In particular the Euler characteristic of Σ must be even.

On the other hand, the Euler characteristic of a degree d complex surface is $d(6 - d(4 - d))$ (This can be proved using the adjunction formula and the fact that the Euler characteristic is equal to the top Chern number: see [8]).   □

In this section we have proved a number of basic topological facts about the discriminant locus, but much remains unanswered. For example can we obtain bounds on the number of connected components of $\mathcal{D}$ or on the number of triple points? One can find crude bounds rather easily using the Milnor–Thom bound ([10, 13]). This states that the sum of the Betti numbers of a real algebraic variety in $\mathbb{R}^m$ defined as the zero set of a finite number of polynomial equations of degree k is less than or equal to

$$k(2k - 1)^{m-1}.$$

Thus for a cubic surface the sum of the Betti numbers of $\mathcal{D}$ is bounded above by $12(23)^3 = 146004$ and the number of triple points is bounded above by $8(15)^3 = 27000$. One can surely do rather better!

Note that for the related question of the number of twistor lines, we have a sharp bound: there are at most 5 twistor lines. See [1] for a proof and a classification of cubic surfaces with 5 twistor lines.

5. The topology of singular surfaces

The primary aim of this paper is to compute the topology of the discriminant locus of the Fermat cubic. But what does it actually mean to compute the topology of a space X? The very notion presupposes that one has a classification theorem for the candidate topologies and one wishes to identify the topology of X within this classification. In order to compute the topology of the discriminant locus, therefore, we need some classification for the topology of singular surfaces. Since we expect that for generic cubics, the discriminant locus will have isolated singularities, let us focus on this case.

Definition 5.1. A topological space is a *real surface with isolated topological singularities* if it is homeomorphic to a finite CW-complex built using only 0, 1 and 2 cells where precisely two faces meet at any given edge. This ensures that along the interior of the edges the space is locally homeomorphic to $\mathbb{R}^2$.

A *topological singularity* is a point on such a surface which is not locally homeomorphic to $\mathbb{R}^2$. We will sometimes abbreviate this to simply *singularity* when there is no danger of confusion with the algebraic notion of singularity. We empahsise the distinction because we will find in practice that the triple points of the Fermat cubic are algebraically singular but not topologically singular.

The topological classification of such spaces is straightforward but perhaps not very well known. We will show how to classify theses spaces by means of an associated graph which encodes the topology. See [7] for an alternative, but equivalent, description for the case of surfaces in $\mathbb{RP}^3$.

Let us begin by describing the associated graph in some special cases, we will then explain more formally how to construct the graph.

For a nonsingular compact real surface, the graph consists of a single node labelled either Σ_g or Θ_c with $g \in \mathbb{N}$ and $c \in \mathbb{N}^+$. Σ_g is the label used for a connected orientable surface of genus g. Θ_n is the label used for a connected nonorientable surface with c cross caps.

When n smooth points of a singular real surface are glued together at a point we add one extra node to the graph representing the glue point. We join this node to the nodes representing the smooth parts of the surface that have been glued together.

Example 5.2. The surface obtained by choosing two points on a sphere, gluing one point to a torus and the other to a Klein bottle has graph:

$$\Sigma_1 — \circ — \Sigma_0 — \circ — \Theta_2.$$

If one takes three points on a sphere and glues them all together, the resulting surface has graph $\Sigma_0 \!\!=\!\!=\!\!= \circ$.

Let us now describe in general how to associate a graph Γ_Δ to a cell decomposition Δ. The point we wish to emphasize is the algorithmic way in which one can compute Γ_Δ from Δ.

First, we need to understand the topology of the surface at the singularities. Given a vertex v of the cell decomposition we can define a graph Γ_v as follows: add a node to the graph for each edge that ends at v; for each face in the cell decomposition which has two edges that meet at v in its boundary, connect the corresponding nodes in the Γ_v. Since two faces meet at each edge, Γ_v will consist simply of closed loops. Let n_v denote the number of loops. If $n_v \neq 0$, the surface is locally homeomorphic to n_v discs whose origins have all been glued together with v corresponding to the glue point. In the case $n_v = 0$ the surface consists of a single point. Note that in the case $n_v = 1$, the surface is locally homeomorphic to $\mathbb{R}^2$.

We can now define the resolution of a singularity to be the cell decomposition obtained by replacing the vertex with n_v vertices each connected to one of the components of Γ_v. This construction simply corresponds to ungluing the discs.

Given a cell decomposition Δ we now define the nodes of the graph Γ_Δ. The nodes of Γ_Δ are defined to be the union of two sets N_1 and N_2. The set of nodes N_1 is given by the set of connected components of the topological space Δ with its vertices removed. By resolving the singularities of each connected component, we obtain a compact smooth real surface. We add the data of its Euler characteristic and orientation to each node in N_1.

The nodes N_2 for Γ_Δ are defined to be the topological singularities. That is they correspond to the vertices of Δ with $n_v \neq 1$. There is no additional data associated with these nodes.

The links in Γ_Δ are defined as follows: we add one link to the node $v \in N_2$ for each connected component of Γ_v; this link connects the node v to the node in N_1 containing the edges and faces of associated with the connected component. There are no other links.

With the obvious notion of graph homomorphism for this category of graphs, the graph Γ_Δ completely classifies the surface up to homeomorphism. This follows from the classification theorem for closed nonsingular surfaces.

We can now state the aim of this paper more clearly. It is to compute the graph that encodes the topology of the discriminant locus of the Fermat cubic.

6. The discriminant locus of the Fermat cubic

The discriminant locus defines a surface in $\mathbb{R}^4 \cup \{\infty\}$ which we can view as the world sheet swept out as a curve moves through $\mathbb{R}^3$. A first step to understanding the discriminant locus is to generate an animation of this curve. One hopes that by careful study of the resulting curve we should be able to piece together the topology of the surface. We will do this in two stages — firstly we will calculate the topology by a simple visual examination of the curve. We will then show how the results of this visual examination can be rigorously justified.

The ease with which one can comprehend the animation of the discriminant locus depends crucially upon the choice of coordinates for $\mathbb{R}^4$. The ideal coordinates for viewing the Fermat cubic are not immediately apparent. As a preliminary step to choosing good coordinates, let us describe the conformal symmetries of the Fermat cubic. This will surely guide our choice of coordinates.

The Fermat cubic is defined by the equation

$$z_1^3 + z_2^3 + z_3^3 + z_4^3 = 0.$$

There is an obvious S^4 action given by permuting the coordinates. One can also make transformations such as $(z_1, z_2, z_3, z_4) \mapsto (\omega_1 z_1, \omega_2 z_2, \omega_3 z_3, \omega_4 z_4)$ where each ω_i is a cube root of unity. These generate all the projective symmetries of the Fermat cubic.

It is easy now to check that the conformal symmetries of the Fermat cubic are generated by

$$(z_1, z_2, z_3, z_4) \mapsto (z_3, z_4, z_1, z_2),$$
$$(z_1, z_2, z_3, z_4) \mapsto (\omega z_1, \omega^2 z_2, z_3, z_4),$$

where $\omega = e^{\frac{2\pi i}{3}}$. Thus the group of conformal symmetries is isomorphic to $\mathbb{Z}_3 \times \mathbb{Z}_2$.

The next observation to make is that the Fermat cubic has three twistor lines. This is easily checked using the well known explicit description for the 27 lines on the Fermat cubic.

If one then chooses coordinates for S^4 such that the twistor lines are at $(-1, 0, 0, 0)$, $(1, 0, 0, 0)$ and ∞ then by Proposition 3.1 the equations for the discriminant locus are equations of degree 8 and the equations for the triple points are of degree 4. The equations for the triple points are sufficiently simple for Mathematica to be able to solve them and it is indeed feasible to solve them by hand. This demonstrates the practical value of Proposition 3.1.

If we then transform back to the standard coordinates we have:

Lemma 6.1. *Identifying S^4 with $\mathbb{H} \cup \{\infty\}$, the triple points for the Fermat cubic have coordinates*

$$-\frac{1}{2}j + \frac{\sqrt{3}}{2}k, \quad \frac{1}{2}j + \frac{\sqrt{3}}{2}k, \quad -j, \quad j, \quad -\frac{1}{2}j - \frac{\sqrt{3}}{2}k, \quad \frac{1}{2}j - \frac{\sqrt{3}}{2}k.$$

The twistor lines for the Fermat cubic lie above the points

$$-1, \quad \frac{1}{2} + \frac{\sqrt{3}}{2}i, \quad \frac{1}{2} - \frac{\sqrt{3}}{2}i.$$

Notice that the triple points all lie on a circle and are conformally equivalent to the 6 roots of unity. We will exploit the six fold symmetry this suggests later.

All 9 points lie in the unit sphere, so we can make a quaternionic Möbius transformation to transform these points so they all lie in the plane $x_1 = 0$. Then, if we produce an animation with time coordinate x_1 we will be able to view all these singular points simultaneously at time $x_1 = 0$.

We make the Möbius transformation is $q \mapsto (q - k)^{-1}(-q - k)$. It transforms the six triple points to the following points: $-(2 + \sqrt{3})i$, $(2 + \sqrt{3})i$, $-i$, i, $-(2 - \sqrt{3})i$, $(2 - \sqrt{3})i$. Note that they all lie on the j axis. The points corresponding to the twistor lines are mapped to $-\frac{\sqrt{3}}{2}j - \frac{1}{2}k$, $+\frac{\sqrt{3}}{2}j - \frac{1}{2}k$ and k. They lie in a circle in the j, k plane.

Let us use the notation $\mathbf{x}'$ for these transformed coordinates. In these coordinates, the animation of the discriminant locus becomes considerably simpler.

The discriminant locus at time $x_1' = 0$:
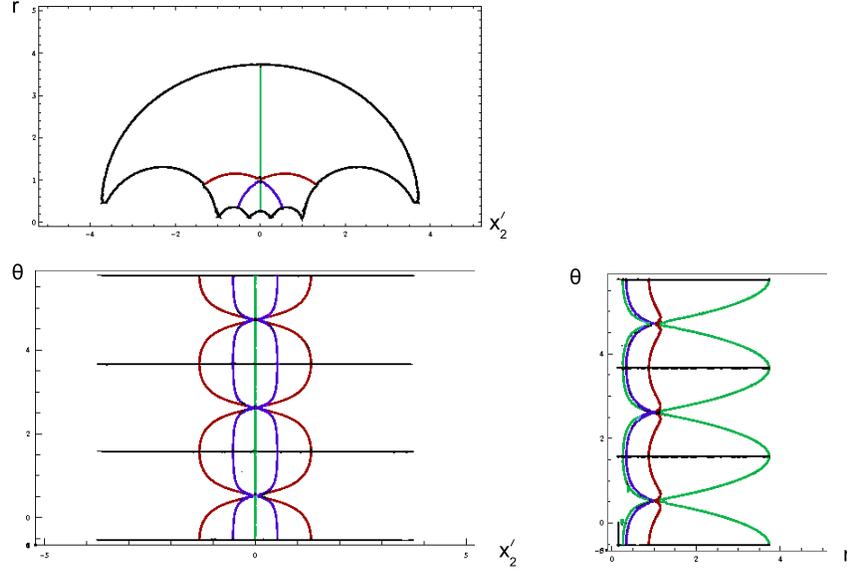
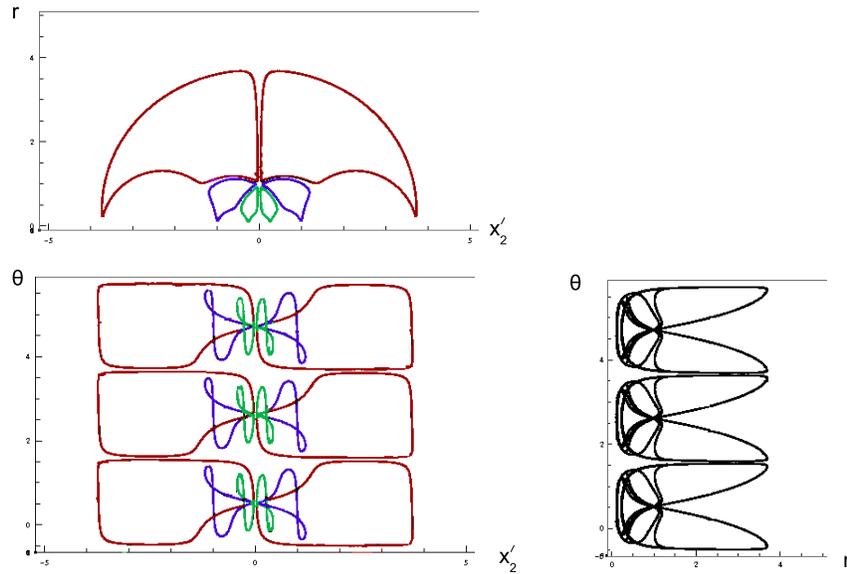The discriminant locus at time $x_1' = 0.02$:

FIGURE 6.1. Three views of the discriminant locus at two different times.

One feature that stands out when using these coordinates is an apparent rotation symmetry given by rotating through 120 degrees about the i axis. This suggests that it might be useful to introduce cylindrical polar coordinates. We write $x_3' = r \cos \theta$ and $x_4' = r \sin \theta$.
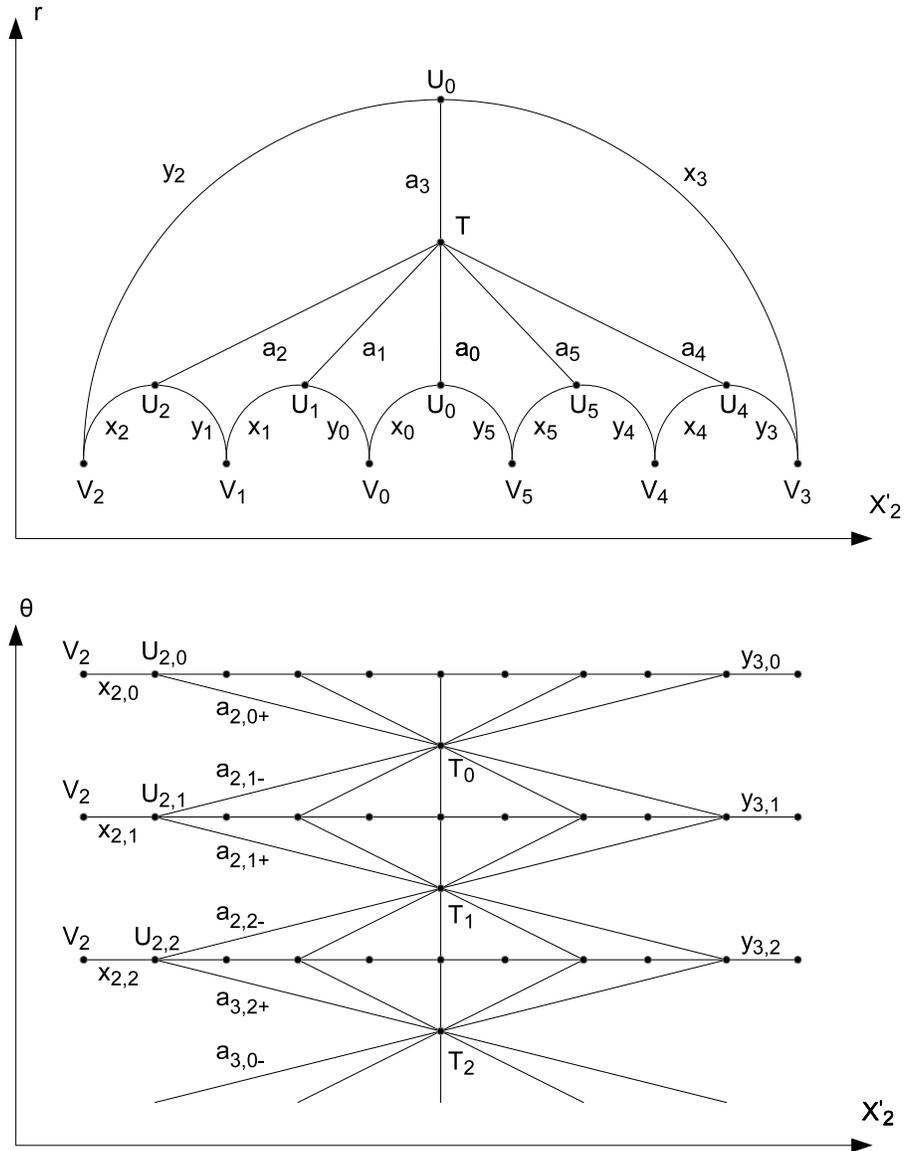
FIGURE 6.2. Labels for the vertices and edges of the cell decomposition.

In Figure 6.1 we have used these cylindrical polar coordinates to plot the discriminant locus at each of the times $x'_1 = 0$ and $x'_1 = 0.02$. We have arranged the pictures so that the reader can (mentally or physically) fold the page to obtain a three dimensional view. We have omitted the points where $r = 0$ since they are a little confusing since points with $r = 0$ need to be identified appropriately in polar coordinates. If we had included the

points there would be six vertical lines representing the triple points running across the front of the figure at time $x_1' = 0$.

For each time point we have coloured the plots to indicate which parts of the different views correspond. We have not coloured the view of the (r, θ) plane at time 0.02 as the nontransverse intersections make it difficult to work out how the curves correspond to the other figures. Note that there is no relationship between the colours used at times $x_1' = 0$ and $x_1' = 0.02$.

The first thing to notice about Figure 6.1 is the translation symmetry on the θ axis (corresponding to 120 degree rotations in the x' coordinates). If one simplifies the expression for the discriminant locus in these coordinates one obtains an expression only involving θ via the functions $\cos(3\theta)$ and $\sin(3\theta)$. This proves the visually apparent symmetry is a genuine symmetry of the discriminant locus.

This is surprising since this symmetry *does not* arise from the group of conformal symmetries $\mathbb{Z}_3 \times \mathbb{Z}_2$ acting on the Fermat cubic. We conclude that the discriminant locus is more symmetrical than the Fermat cubic itself. We will discover as we continue our study that it has yet more symmetries.

Next note that at small positive $x_1' > 0$ times the discriminant locus consists of a number of disjoint loops. We have illustrated this behaviour with only one time point $x_1' = 0.02$, but it appears to be true for all positive times when one plots an animation. As time progresses, each of these loops shrinks to a point and then disappears. There is a time symmetry in these coordinates which ensures that at small negative times, one similarly sees a number of disjoint loops which shrink to a point and then disappear as time x_1' decreases.

Since the worldsheet of a loop shrinking to a point and disappearing is homeomorphic to $\mathbb{R}^2$, this suggests that we have found a cell decomposition of the discriminant locus.

The vertices and edges of the cell decomposition are given by the curve at time $x_1' = 0$. Plotting the curve at this time does indeed show it to be singular: the singularities are the vertices of our cell decomposition, the smooth curves are the edges. The worldsheets of the loops at positive and negative times give the faces of our cell decomposition.

Note that the view of the (x_2', r) plane clearly shows 6 distinct loops at time $t = 0.02$. As time progresses these loops shrink to points and disappear. Taking into account the $\mathbb{Z}_3$ symmetry, this gives a total of 18 loops for positive times. There is also a time symmetry given by

$$(x_1', x_2', r, \theta) \mapsto (-x_1', -x_2', r, \theta).$$

Thus we have identified a cell decomposition with 36 faces.

So, by means of visual inspection, we have identified a cell decomposition of the discriminant locus. We have two tasks remaining: the first is to compute the topology of the discriminant locus from the cell decomposition; the second is to rigorously justify the existence of the cell decomposition.

The first task is reasonably simple. We postpone the second to the next section.

Proposition 6.2. *Assuming the cell decomposition of the discriminant locus of the Fermat cubic obtained by visual inspection is correct, its topology is encoded by the graph*:

$$\Sigma_4$$
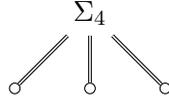
Proof. We label the edges and vertices of the cell decomposition as shown in Figure 6.2.

In the top part of Figure 6.2 we have shown how to associate labels for the edges and vertices seen in the view of the (x_2', r) plane at time $x_1' = 0$. We have used a more schematic representation of the decomposition than that shown in Figure 6.1, but the relationship between the pictures should be obvious. We have used lower case letters to indicate edges. We have used upper case letters to indicate vertices. We have used indices from 0 to 5 to correspond to the approximate rotational symmetry about the point $(0, 1)$ in the (x_2', r) plane. Our numbering starts at the downward pointing vertical and then moves clockwise.

Since the (x_2', r) plane is only two dimensional, some of the edges and vertices of our cell decomposition coincide when viewed in the (x_2', r) plane. We have shown in the lower part of Figure 6.2 how to add a second index to the edges and vertices to indicate their θ coordinate. In summary then our edges and vertices can be enumerated as follows:

- Edges $a_{i,j}$ $i \in \{0, 1, 2, 3, 4, 5\}$, $j \in \{0+, 1-, 1+, 2-, 2+, 0-\}$;
- Edges $x_{i,j}$ $i \in \{0, 1, 2, 3, 4, 5\}$, $j \in \{0, 1, 2\}$;
- Edges $y_{i,j}$ $i \in \{0, 1, 2, 3, 4, 5\}$, $j \in \{0, 1, 2\}$;
- Vertices $U_{i,j}$ $i \in \{0, 1, 2, 3, 4, 5\}$, $j \in \{0, 1, 2\}$;
- Vertices V_i $i \in \{0, 1, 2, 3, 4, 5\}$;
- Vertices T_j $j \in \{0, 1, 2\}$.

Notice that we only have 6 vertices of the form V_i since when $r = 0$ we must identify points that only differ by the value of θ.

We label the faces of our cell decomposition $f_{i,j}^{\pm}$ with $i \in \{0, 1, 2, 3, 4, 5\}$ and $j \in \{0, 1, 2\}$. Here the plus or minus indicates whether the face corresponds to positive times $x_1' > 0$ or to negative times. The i index indicates the sector of the (x_2', r) plane and the j indicates the values of θ in accordance with the conventions used for edges and vertices.
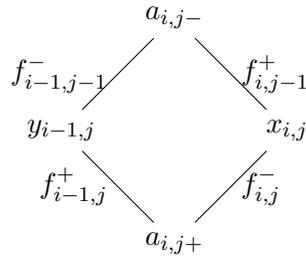
An examination of Figure 6.1 allows us to write down the boundary of each face:

$$\partial(f_{i,j}^+) = x_{i,j+1} + a_{i,(j+1)-} + a_{i+1,j+} + y_{i,j},$$
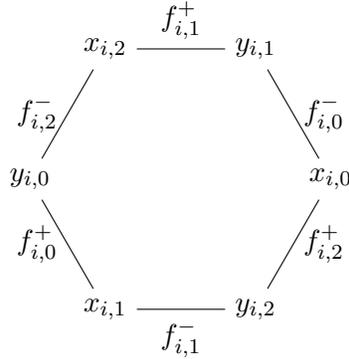$$\partial(f_{i,j}^-) = x_{i,j} + a_{i,j+} + a_{i+1,(j+1)-} + y_{i,j+1}.$$

In the formulae above, arithmetic in indices is performed modulo 6 when working with the i indices and modulo 3 when working with the j indices. We will use modular arithmetic for i and j indices for the rest of the proof without further comment.

One can see immediately from the above formulae for the faces in our cell decomposition that precisely two faces meet at each edge. Thus the cell decomposition describes a surface with isolated topological singularities.
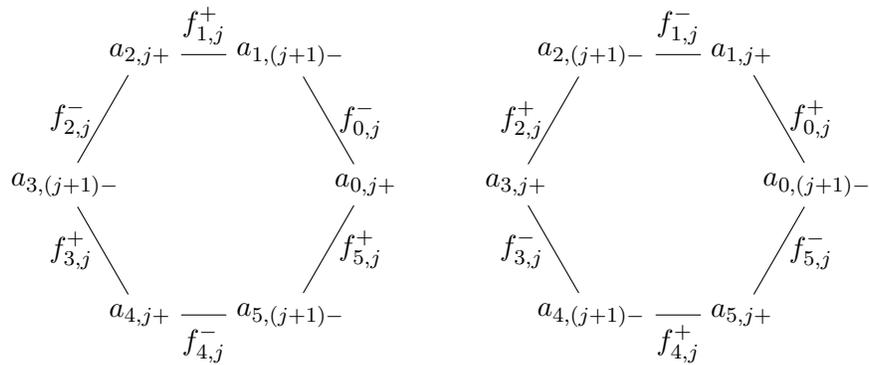
We compute the local topology at a vertex v by drawing the graph Γ_v as described in Section 4. The graph $\Gamma_{U_{i,j}}$ is:

$$
\begin{array}{ccc}
& a_{i,j-} & \\
f^-_{i-1,j-1} \nearrow & & \nwarrow f^+_{i,j-1} \\
y_{i-1,j} & & x_{i,j} \\
f^+_{i-1,j} \searrow & & \swarrow f^-_{i,j} \\
& a_{i,j+} &
\end{array}
$$

The graph Γ_{V_i} is:

$$
\begin{array}{ccc}
& x_{i,2} \;\overset{f^+_{i,1}}{\text{———}}\; y_{i,1} & \\
f^-_{i,2} \nearrow & & \nwarrow f^-_{i,0} \\
y_{i,0} & & x_{i,0} \\
f^+_{i,0} \searrow & & \swarrow f^+_{i,2} \\
& x_{i,1} \;\underset{f^-_{i,1}}{\text{———}}\; y_{i,2} &
\end{array}
$$

The graph Γ_{T_j} is:

$$
\begin{array}{ccc}
a_{2,j+} \;\overset{f^+_{1,j}}{\text{———}}\; a_{1,(j+1)-} & & a_{2,(j+1)-} \;\overset{f^-_{1,j}}{\text{———}}\; a_{1,j+} \\
f^-_{2,j} \nearrow \qquad\qquad \searrow f^-_{0,j} & & f^+_{2,j} \nearrow \qquad\qquad \searrow f^+_{0,j} \\
a_{3,(j+1)-} \qquad\qquad a_{0,j+} & & a_{3,j+} \qquad\qquad a_{0,(j+1)-} \\
f^+_{3,j} \searrow \qquad\qquad \nearrow f^+_{5,j} & & f^-_{3,j} \searrow \qquad\qquad \nearrow f^-_{5,j} \\
a_{4,j+} \;\underset{f^-_{4,j}}{\text{———}}\; a_{5,(j+1)-} & & a_{4,(j+1)-} \;\underset{f^+_{4,j}}{\text{———}}\; a_{5,j+}
\end{array}
$$

We deduce that the discriminant locus has precisely three topological singularities T_0, T_1 and T_2 corresponding to the twistor lines. At these singularities, the discriminant locus is locally homeomorphic to two discs glued together at a point.

Since the faces $f_{i,j}^+$ and $f_{i,j}^-$ lie in a connected component component of the graph Γ_{V_i}, these faces can be connected via a path that avoids all vertices. The graph Γ_{V_i} also shows that the faces $f_{i,j_1}^\pm$ and $f_{i,j_2}^\pm$ can be connected by such a path for all j_1 and j_2. Similarly the graph of Γ_{T_j} shows that the faces $f_{i_1,j}^\pm$ and $f_{i_2,j}^\pm$ can be connected by such a path for all i_1 and i_2. We deduce that all faces can be connected by a path that avoids the singularities.

We know from Proposition 4.2 that discriminant locus is orientable away from the triple points and twistor lines. We deduce from this and the considerations above that the topology of the discriminant locus is described by a graph of the form:
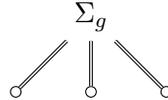
Our cell decomposition contains 27 vertices, 72 edges and 36 faces so has Euler characteristic -9. One can alternatively calculate this using Lemma 6.1 and Proposition 4.4. The Euler characteristic of the singular surface associated with the graph above is $(2 - 2g) - 3$. So $g = 4$. $\square$

7. Symmetry of the discriminant locus

The first step towards a rigorous justification of the above results is to find a simpler expression for the discriminant locus. To do this we need to exploit all of its symmetries.

Assuming that our topological calculation above is correct, one sees that the image of the twistor lines on the Fermat cubic's discriminant locus can be identified entirely in terms of the geometry of the discriminant locus without reference to the Fermat cubic. They are simply the points of the discriminant locus that are not locally homeomorphic to $\mathbb{R}^2$. Thus any conformal symmetry of the discriminant locus must preserve the 3 points corresponding to the twistor lines.

Similarly one can identify the triple points as the points of the discriminant locus that are not smoothly embedded in S^4 yet are locally homeomorphic to $\mathbb{R}^2$. Thus any conformal symmetry of the discriminant locus must preserve the 6 triple points. We can use this to put a bound on the size of the group of conformal symmetries of the discriminant locus of the Fermat cubic.

Lemma 7.1. *The group, G, of conformal symmetries that permute the six triple points of the Fermat cubic and its three twistor lines is isomorphic to $D_3 \times D_6$.*

Proof. By Lemma 6.1, we have identified a round 3-sphere in S^4 that contains all 9 nonsmooth points. It is the unique such sphere, so it too must be preserved by any element of G. There is a one to one correspondence between conformal symmetries of $\mathbb{R}^4$ that leave this 3-sphere fixed and angle preserving (but not necessarily orientation preserving) symmetries of the 3-sphere.

The six triple points all lie on a hexagon in the unit circle in the plane spanned by the quaternions j and k and the three twistor lines lie on an equilateral triangle in the unit circle in the plane spanned by 1 and and i. The symmetry group of a regular n-gon in the plane is D_n. Thus we can find a subgroup $D_3 \times D_6$ of $\subset O(2) \times O(2) \subset O(4)$ acting on $\mathbb{R}^4$ which preserves the twistor lines and triple points. The induced maps on the unit sphere S^3 are isometries and hence angle preserving. Thus G contains $D_3 \times D_6$.

To show that there are no further symmetries, we switch to the $\mathbf{x}'$ coordinates. The unit 3-sphere becomes the hyperplane $x_1' = 0$ together with the point at infinity. Let C_3 be the unit circle in the $x_1' = x_2' = 0$ plane containing the image of the twistor lines. Let C_6 be the line $x_1' = x_3' = x_4' = 0$ containing all 6 triple points.

We can make a further conformal change of coordinates on the three sphere that fixes C_3 and C_6 but which moves one of the triple points to infinity and another to zero. In these coordinates, any quaternionic Möbius transformation that fixes the triple points must be given by a linear map. This map must be conformally equivalent to a unitary map. If this map also fixes C_3 it must be an isometry. Thus the group of transformations that fix C_6 and permute C_3 is D_3.

We can make a conformal transformation of the three spheres that swaps C_3 and C_6. The argument above then shows that the group of transformations that fix C_3 and permute C_6 is the dihedral group D_6. The result follows. □

Lemma 7.2. *The discriminant locus of the Fermat cubic is invariant under* G.

Proof. Making the coordinate change

$$x_1 = a \cos \alpha, \quad x_2 = a \sin \alpha, \quad x_3 = b \cos \beta, \quad x_4 = b \sin \beta$$

and simplifying yields the following equations for discriminant locus of the Fermat cubic:

$$(7.1) \quad -2a^3 \cos(3\beta) \sin(3\alpha) + (-1 + a^6 + 3a^4b^2 + 3a^2b^4 + b^6) \sin(3\beta) = 0,$$

$$(7.2) \quad 1 + 4a^6 - 4b^6 + a^{12} + b^{12} + 6a^4b^2 - 6a^2b^4 + 6a^{10}b^2 + 6a^2b^{10} +$$
$$15a^8b^4 + 15a^4b^8 + 20a^6b^6 + 2b^6 \sin(6\beta) + 2a^6 \cos(6\alpha) +$$
$$4a^3(1 + a^6 + b^6 + 3a^4b^2 + 3a^2b^4) \cos(3\alpha) = 0.$$

The invariance of the discriminant locus under the rotations

$$\mathbb{Z}_3 \times \mathbb{Z}_6 \subset D_3 \times D_6$$

is now manifest.

Under the transformation

$$a \mapsto a/(a^2 + b^2), \quad b \mapsto b/(a^2 + b^2), \quad \alpha \mapsto -\alpha, \quad \beta \mapsto \beta,$$

these two equations are transformed to nonzero multiples of themselves. So the discriminant locus is invariant under this transformation. Similarly it is invariant under the transformation

$$a \mapsto a/(a^2 + b^2), \quad b \mapsto b/(a^2 + b^2), \quad \alpha \mapsto \alpha, \quad \beta \mapsto -\beta.$$

Together these transformations generate G. □

Although the coordinates used in the above lemma give the simplest explanation for the symmetries of the discriminant locus, the topology seems easier to understand in the x' coordinates. This is because all the vertices of the cell decomposition can be viewed at the single time $x'_1 = 0$. It is by combining the best features of both coordinate systems that we will be able to certify the topology of the discriminant locus. Therefore, let us consider the equations for the discriminant locus in the cylindrical polar coordinates used in the previous section. The equations take form:

(7.3) $$p_1(r, x'_1, x'_2) + r^6 \cos(6\theta) + p_2(r, x'_1, x'_2) \sin(3\theta) = 0,$$

(7.4) $$p_3(r, x'_1, x'_2) + p_4(r, x'_1, x'_2) \cos(3\theta) = 0,$$

for some polynomials p_1, p_2, p_3 and p_4. So long as $p_4 \neq 0$ we can solve for $\cos(3\theta)$ using Equation (7.4). We can then substitute the resulting value for $\cos(6\theta) = 2\cos(3\theta)^2 - 1$ into Equation (7.3) and hence solve for $\sin(3\theta)$, assuming $p_2 \neq 0$.

$$\cos(3\theta) = -\frac{p_3}{p_4},$$

$$\sin(3\theta) = \frac{r^6(p_4^2 - 2p_3^2) - p_4^2 p_1}{p_2 p_4^2}.$$

These equations have a unique solution for $\theta \in [0, \frac{2\pi}{3})$ so long as the sum of the squares of the right hand sides is equal to 1. Thus away from the points where $p_4 = 0$ or $p_2 = 0$ we see that the discriminant locus is a triple cover of the surface defined by the equation:

(7.5) $$p_2^2 p_3^2 p_4^2 + (r^6(1 - 2p_3^2) - p_4^2 p_1)^2 = p_2^2 p_4^4$$

and the inequality

(7.6) $$r \geq 0.$$

Excluding the cases where $p_4 = 0$ or $p_2 = 0$, we have reduced our problem from one of considering the intersection of two polynomials in $\mathbb{R}^4$ to a problem involving the zero set of a single polynomial in $\mathbb{R}^3$. This is a

considerable simplification since the topology of surface defined by a single equation is much easier to understand than a surface defined by two equations. Having said that, the degree of Equation (7.5) is 44. One also needs to give careful consideration to the situation when $p_4 = 0$ or $p_2 = 0$. We omit the details, but one can, with the aid of computer algebra, prove all solutions with $p_4 = 0$ or $p_2 = 0$ in fact satisfy Equation (7.5).

We now make a conformal transformation of Equation (7.5) sending the six triple points to a circle. We transform to new coordinates $((x, y, t))$ as follows:

$$r = \frac{1 - x^2 - y^2 - t^2}{x^2 + t^2 + (1 - y)^2},$$

$$x_1' = \frac{2t}{x^2 + t^2 + (1 - y)^2},$$

$$x_2' = \frac{2x}{x^2 + t^2 + (1 - y)^2}.$$

The inequality (7.6) transforms under this coordinate change to the condition $x^2 + y^2 + t^2 \leq 1$. After this transformation, a D_6 symmetry does indeed become clear. We once again introduce cylindrical polar coordinates $y = R \sin \phi$, $u_2 = R \cos \phi$. The inequality (7.6) becomes $R^2 + t^2 \leq 1$. Equation (7.5) takes the form:

$$(7.7) \qquad \sum_{n \in \{6,12,18,24\}} p_n(R, t) R^{12} \cos(n\phi)$$

for appropriate polynomials p_n.

We write $\cos(6\phi) = \Phi$ for a new coordinate $\Phi \in [-1, 1]$. With this coordinate change (7.5) becomes a quartic in Φ with coefficients that are polynomials in R and u_1. The discriminant locus will be a $3 \times 12 = 36$ sheeted cover of the implicit surface obtained.

It turns out these coefficients are of entirely even degree in both R and t. So we make another simplification and introduce new variables (S, T) with $S = R^2$ and $T = t^2$ with the conditions $S \geq 0$ and $x \geq 0$. Note that this indicates another symmetry of the discriminant locus given by the map $t- > -t$.

By means of these algebraic manipulations we have now confirmed that G preserves the discriminant locus and simultaneously introduced simpler coordinates.

The final change of coordinates is to write $Z = S + T$ and work with the coordinates (Z, Φ, T). This final change of coordinates is designed so that (7.6) transforms to the simple condition $Z \leq 1$.

In summary then, we have introduced new coordinates (T, Z, Φ) such that the discriminant locus is a 72 sheeted cover of the implicit surface defined

by the inequalities:

$$(7.8) \qquad\qquad T \geq 0, \quad 0 \leq Z \leq 1, \quad -1 \leq \Phi \leq 1$$

and the transformed equation (7.5). The transformed equation will be of degree 4 in Φ.

We know from Equation (7.7) that there is a constant factor of R^{12} that we can cancel. After making this cancellation and also the cancellation of a constant factor, one obtains the equation:

(7.9)

$426T^2 - 228\Phi T^2 - 6\Phi^2 T^2 + 3792T^3 - 496\Phi T^3 - 848\Phi^2 T^3 - 16\Phi^3 T^3 + 7584T^4 + 96\Phi T^4 - 1056\Phi^2 T^4 - 480\Phi^3 T^4 + 4608T^5 + 1536\Phi T^5 + 1536\Phi^2 T^5 - 1536\Phi^3 T^5 + 128T^6 + 1024\Phi T^6 + 1792\Phi^2 T^6 - 1024\Phi^3 T^6 + 128\Phi^4 T^6 + 228TZ + 240\Phi TZ + 12\Phi^2 TZ + 3936T^2 Z + 432\Phi T^2 Z + 1728\Phi^2 T^2 Z + 48\Phi^3 T^2 Z + 22944T^3 Z - 288\Phi T^3 Z - 1056\Phi^2 T^3 Z + 1440\Phi^3 T^3 Z + 31104T^4 Z - 384\Phi T^4 Z - 1920\Phi^2 T^4 Z + 1920\Phi^3 T^4 Z + 8448T^5 Z + 4608\Phi^2 T^5 Z - 768\Phi^4 T^5 Z - 6Z^2 - 12\Phi Z^2 - 6\Phi^2 Z^2 + 912TZ^2 + 48\Phi TZ^2 - 912\Phi^2 TZ^2 - 48\Phi^3 TZ^2 + 13368T^2 Z^2 + 1968\Phi T^2 Z^2 + 5304\Phi^2 T^2 Z^2 - 1440\Phi^3 T^2 Z^2 + 55344T^3 Z^2 - 3600\Phi T^3 Z^2 - 3504\Phi^2 T^3 Z^2 + 3600\Phi^3 T^3 Z^2 + 47424T^4 Z^2 - 5568\Phi T^4 Z^2 - 10176\Phi^2 T^4 Z^2 + 3264\Phi^3 T^4 Z^2 + 1920\Phi^4 T^4 Z^2 + 4608T^5 Z^2 + 1536\Phi T^5 Z^2 + 1536\Phi^2 T^5 Z^2 - 1536\Phi^3 T^5 Z^2 + 16\Phi Z^3 + 32\Phi^2 Z^3 + 16\Phi^3 Z^3 + 1872TZ^3 - 1824\Phi TZ^3 - 3216\Phi^2 TZ^3 + 480\Phi^3 TZ^3 + 27168T^2 Z^3 + 4176\Phi T^2 Z^3 + 6336\Phi^2 T^2 Z^3 - 6960\Phi^3 T^2 Z^3 + 74944T^3 Z^3 - 1472\Phi T^3 Z^3 - 4544\Phi^2 T^3 Z^3 + 192\Phi^3 T^3 Z^3 - 2560\Phi^4 T^3 Z^3 + 31104T^4 Z^3 - 384\Phi T^4 Z^3 - 1920\Phi^2 T^4 Z^3 + 1920\Phi^3 T^4 Z^3 + 24Z^4 + 48\Phi Z^4 + 24\Phi^2 Z^4 + 3696TZ^4 - 1584\Phi TZ^4 - 2160\Phi^2 TZ^4 + 3120\Phi^3 TZ^4 + 35004T^2 Z^4 + 8808\Phi T^2 Z^4 + 12444\Phi^2 T^2 Z^4 - 4800\Phi^3 T^2 Z^4 + 1920\Phi^4 T^2 Z^4 + 55344T^3 Z^4 - 3600\Phi T^3 Z^4 - 3504\Phi^2 T^3 Z^4 + 3600\Phi^3 T^3 Z^4 + 7584T^4 Z^4 + 96\Phi T^4 Z^4 - 1056\Phi^2 T^4 Z^4 - 480\Phi^3 T^4 Z^4 - 144\Phi Z^5 - 288\Phi^2 Z^5 - 144\Phi^3 Z^5 + 4248TZ^5 - 2976\Phi TZ^5 - 4344\Phi^2 TZ^5 + 2112\Phi^3 TZ^5 - 768\Phi^4 TZ^5 + 27168T^2 Z^5 + 4176\Phi T^2 Z^5 + 6336\Phi^2 T^2 Z^5 - 6960\Phi^3 T^2 Z^5 + 22944T^3 Z^5 - 288\Phi T^3 Z^5 - 1056\Phi^2 T^3 Z^5 + 1440\Phi^3 T^3 Z^5 + 92Z^6 + 184\Phi Z^6 + 220\Phi^2 Z^6 + 256\Phi^3 Z^6 + 128\Phi^4 Z^6 + 3696TZ^6 - 1584\Phi TZ^6 - 2160\Phi^2 TZ^6 + 3120\Phi^3 TZ^6 + 13368T^2 Z^6 + 1968\Phi T^2 Z^6 + 5304\Phi^2 T^2 Z^6 - 1440\Phi^3 T^2 Z^6 + 3792T^3 Z^6 - 496\Phi T^3 Z^6 - 848\Phi^2 T^3 Z^6 - 16\Phi^3 T^3 Z^6 - 144\Phi Z^7 - 288\Phi^2 Z^7 - 144\Phi^3 Z^7 + 1872TZ^7 - 1824\Phi TZ^7 - 3216\Phi^2 TZ^7 + 480\Phi^3 TZ^7 + 3936T^2 Z^7 + 432\Phi T^2 Z^7 + 1728\Phi^2 T^2 Z^7 + 48\Phi^3 T^2 Z^7 + 24Z^8 + 48\Phi Z^8 + 24\Phi^2 Z^8 + 912TZ^8 + 48\Phi TZ^8 - 912\Phi^2 TZ^8 - 48\Phi^3 TZ^8 + 426T^2 Z^8 - 228\Phi T^2 Z^8 - 6\Phi^2 T^2 Z^8 + 16\Phi Z^9 + 32\Phi^2 Z^9 + 16\Phi^3 Z^9 + 228TZ^9 + 240\Phi TZ^9 + 12\Phi^2 TZ^9 - 6Z^{10} - 12\Phi Z^{10} - 6\Phi^2 Z^{10} = 0.$

Ugly though this formula is, from a computational complexity viewpoint it is a simplification of Equations (7.1) and (7.2). We started with two degree 12 polynomials in 4 variables and have reduced the problem to a single degree 12 polynomial in 3 variables. Moreover, the polynomial is of degree 4 in one of those variables.

A plot of the surface defined by these conditions is shown in Figure 7.1. Since we introduced $S = R^2$ where R is a radial coordinate, one needs to identify certain points with $S = 0$. Thus a fundamental domain of G is given by an appropriate quotient of Figure 7.1.

We have identified a group of order 72 acting on the discriminant locus. Figure 7.1 represents a fundamental domain of this group action.

The cell decomposition used in the proof of Proposition 6.2 only had 36 faces. To obtain the 72 faces associated with G, one divides each face in
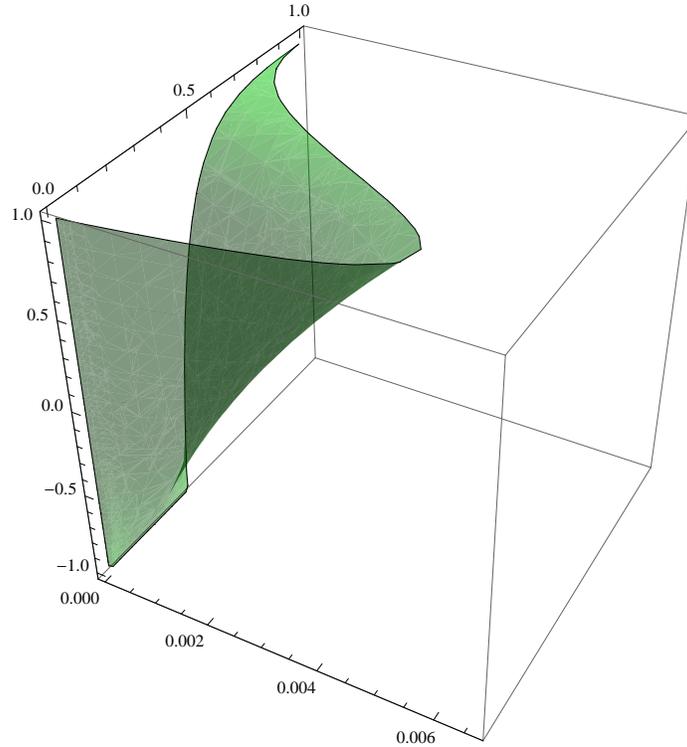
FIGURE 7.1. The surface defined by Equations (7.8) and (7.9).

the cell decomposition used earlier into two pieces by introducing new edges from the twistor lines T_j to the triple points V_i. With this understood, the proof of Proposition 6.2 amounts to a computation of the topology of the tiling of the covering space with copies of this fundamental domain.

8. Cylindrical algebraic decomposition of the fundamental domain

We now wish to:

(1) Identify the points on Figure 7.1 that correspond to points with non trivial stabilizer under G and confirm that they split into vertices and edges homeomorphic to $[0, 1]$ as expected.
(2) Show that the Figure 7.1, with the appropriate quotients when $S = 0$, is homeomorphic to the closed unit disc with boundary given by the points with non trivial stabilizer under G.

If we can complete these tasks we will have rigorously identified a cell decomposition of the discriminant locus.

We begin with the first part. By construction of our coordinate system, the points with non zero stabilizer are points with $S = 0$, $\Phi = -1$, $T = 0$,

$\Phi = 1$. Simplifying Equation (7.9) for each of the first three cases one obtains the following simple equations:

$$(8.1) \qquad\qquad 8T^2(3 + 10T + 3T^2)^4 = 0$$

$$(8.2) \qquad\qquad 8T^2(3 + 3S^2 + 10T + 3T^2 + 6S(1 + T))^4 = 0$$

$$(8.3) \quad 2(1 + \Phi)^2 Z^2(-3 + 12Z^2 + 46Z^4 + 64\Phi^2 Z^4$$
$$+ 12Z^6 - 3Z^8 + 8\Phi(Z - 9Z^3 - 9Z^5 + Z^7)) = 0.$$

The first equation has solutions $T = 0$, $\Phi \in [-1, 1]$. The second equation has the unique solution $S = T = 0$. The third is quadratic in Φ so is also easily understood. All of these solutions have in common the fact that $T = 0$. So referring back to Figure 6.1 these solutions correspond to the edges shown at time $x'_1 = 0$.

The solutions of the equation $\Phi = 1$ correspond to edges used to split the cell decomposition consisting of 36 faces into one of 72 faces. The equation in this case is a little more complex, but does factor into two cubics in T:

$$(8.4) \quad 8(1 + 12T + 24T^2 + 16T^3 + 36TZ + 48T^2Z - 6Z^2 + 36TZ^2 + 24T^2Z^2 + 8Z^3 + 60TZ^3 - 3Z^4) \times$$
$$(24T^2 + 16T^3 + 60TZ + 48T^2Z - 3Z^2 + 36TZ^2 + 24T^2Z^2 + 8Z^3 + 36TZ^3 - 6Z^4 + 12TZ^4 + Z^6)$$
$$= 0.$$

We need to show that the curve defined by this equation together with the conditions $0 \le Z \le 1$ and $0 \le T \le 1$ is homeomorphic to $[0, 1]$. One could do this with one's bare hands, but we will instead discuss how one can use the "cylindrical algebraic decomposition" algorithm.

Cylindrical algebraic decomposition is a foundational algorithm in computational real algebraic geometry. It is an algorithm that allows one to decompose a semi-algebraic set (that is a real set defined by polynomial equalities and inequalities) into pieces called cylindrical sets which are all homeomorphic to either $\{0\}$ or $\mathbb{R}^i$ for some i. In effect, it computes a CW complex that is guaranteed to be homeomorphic to the semi-algebraic set. See [4] for more information.

There is a catch: the running time of cylindrical algebraic decomposition is of the order $(sd)^{c^{n-1}}$ where s is the number of equations and inequations used to define the semi-algebraic set, n is the number of variables, d is the maximum degree of the polynomials and c is a constant. This doubly exponential running time means that cylindrical algebraic decomposition is only effective for rather small problems.

Fortunately the semi-algebraic set defined by (8.4) and $0 \le Z \le 1$ and $0 \le T \le 1$ is appropriately small and one can perform the cylindrical algebraic decomposition quickly. The algorithm works inductively by using resultants to project the equations along each of the coordinate axes to obtain lower dimensional equations. Thus the specific cylindrical decomposition depends upon the semi-algebraic set and the ordering of the coordinate axes. For
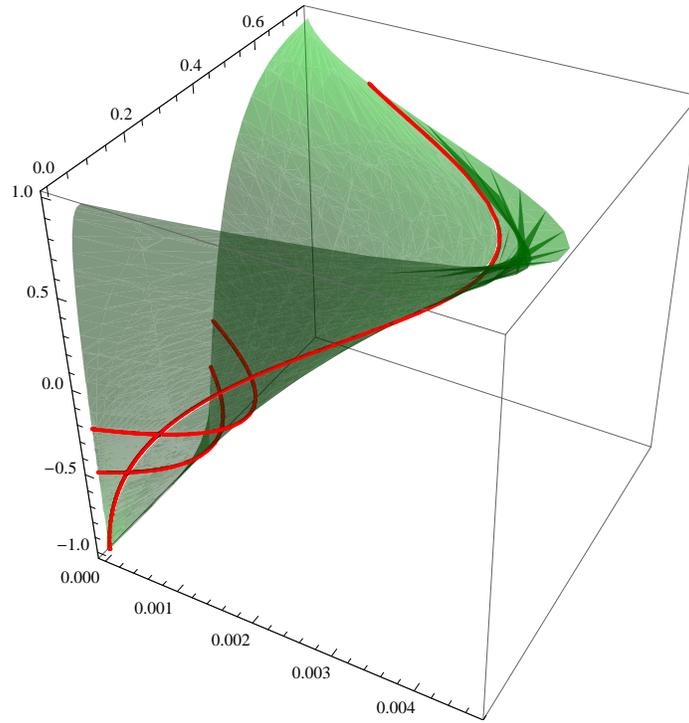
FIGURE 8.1. Cylindrical algebraic decomposition of the fundamental domain.

this case, if one chooses the order (Z, T) one obtains a decomposition into the following three cylindrical sets:

$$\{(0, 0)\},$$
$$\{(1, 0)\},$$
$$\{(Z, T) : 0 < Z < 1 \text{ and } T = \text{root}_\lambda(-3Z^2 + 8Z^3 - 6Z^4 + Z^6 +$$
$$(60Z + 36Z^2 + 36Z^3 + 12Z^4)\lambda + (24 + 48Z + 24Z^2)\lambda^2 + 16\lambda^3, 3)\}.$$

Here we are using the notation $\text{root}_\lambda(p(\lambda), n)$ to denote the nth real root of a polynomial p in the variable λ. We conclude that the semi-algebraic set defined by Equation (8.4) and $0 \le Z \le 1$ and $0 \le T \le 1$ is homeomorphic to $[0, 1]$ as required.

The final ingredient required to complete the proof is to show that the semi-algebraic set defined by Equations (7.8) and (7.9) together with the appropriate quotienting when $S = 0$ is homeomorphic to the closed disc and that its boundary consists of the stabilizer just identified. Using Mathematica we do this by computing the cylindrical algebraic decomposition with respect to the variable ordering Φ, Z, T. The computation takes several minutes to run. Notice that our many simplifications of the equations defining the discriminant locus are crucial to achieving this. For example

simply failing to introduce the coordinate $Z = S + T$ is enough to prevent the algorithm running to completion on our computers.

Since the cylindrical algebraic decomposition in this case is far too lengthy to print out, we have simply plotted the decomposition in Figure 8.1. It consists of six faces. As we saw in the example above, the specific formulae in the cylindrical algebraic decomposition are irrelevant for our purposes. All that matters is the topology implied by the decomposition. Thus the picture in Figure 8.1 summarises all the key information we need about the cylindrical algebraic decomposition. We conclude that our fundamental domain is homeomorphic to 6 closed discs glued as indicated. Hence it is homeomorphic to a disc. Thus the cylindrical algebraic decomposition provides rigorous confirmation of what was visually obvious in Figure 7.1.

We summarize our findings which confirm Proposition 6.2:

Theorem 8.1. *The discriminant locus of the Fermat cubic has topology represented by the graph*:
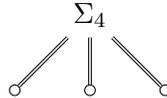

It has conformal symmetry group $D_3 \times D_6$.

In [2] a less formal computation is given for the discriminant locus of the cubic:

$$z_1^2 z_4 + z_4^2 z_1 + z_2^2 z_3 + z_3^2 z_2 = 0.$$

This is called the *transformed Fermat cubic* since it is projectively equivalent but not conformally equivalent to the Fermat cubic. According to the visual examination of the discriminant locus carried out in [2] this has topology given by the graph:

.
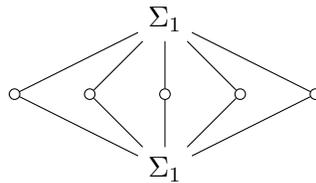
Unfortunately we are not able to reduce the problem to a computationally feasible cylindrical algebraic decomposition in this case, so the result is not fully rigorous. The five topological singularities in this graph correspond to five twistor lines on the transformed Fermat cubic.

It seems that the local topology at the twistor lines is the same for both the rotated Fermat cubic and the Fermat cubic. Likewise the local topology at the triple points is the same in both cases. It would be very interesting if one could catalogue in full the possible topologies at twistor lines and triple points on a nonsingular cubic surface and thereby develop a more extensive theory of twistor cubic surfaces.

References

[1] Armstrong, John; Povero, Massimiliano; Salamon, Simon. Twistor lines on cubic surfaces. *Rend. Sem. Mat. Univ. Pol. Torino.* **71** (2012), no. 3–4, 317–338. arXiv:1212.2851.

[2] Armstrong, John; Salamon, Simon. Twistor topology of the Fermat cubic. *SIGMA* **10** (2014), Paper 061, 12 pp. MR3226989, Zbl pre06334464, arXiv:1310.7150, doi: 10.3842/SIGMA.2014.061.

[3] Atiyah, M. F. Geometry of Yang–Mills fields. *Mathematical problems in theoretical physics* (Proc. Internat. Conf., Univ. Rome, Rome, 1977), pp. 216–221, Lecture Notes in Phys., 80. *Springer, Berlin-New York*, 1978. MR0518436 (80a:14006), Zbl 0435.58001, doi: 10.1007/3-540-08853-9_18.

[4] Basu, Saugata; Pollack, Richard; Roy, Marie-Françoise. Algorithms in real algebraic geometry. Second edition. Algorithms and Computation in Mathematics, 10. *Springer-Verlag, Berlin*, 2006. x+662 pp. ISBN: 978-3-540-33098-1; 3-540-33098-4. MR2248869 (2007b:14125), Zbl 1102.14041, doi: 10.1007/3-540-33099-2.

[5] Bossière, Samuel; Sarti, Alessandra. Counting lines on surfaces. *Ann. Sc. Norm. Super. Pisa Cl. Sci.* (5) **6** (2007), no. 1, 39–52. MR2341513 (2008e:14074), Zbl 1150.14013, arXiv:math/0606100.

[6] Dubé, Thomas W. The structure of polynomial ideals and Gröbner bases. *SIAM J. Comput.* **19** (1990), no. 4, 750–773. MR1053942 (91h:13021), Zbl 0697.68051, doi: 10.1137/0219053.

[7] Fortuna, E.; Gianni, P.; Luminati, D. Effective methods to compute the topology of real algebraic surfaces with isolated singularities. *University of Trento*, (2005). `http://eprints.biblio.unitn.it/844/1/UTM687.pdf`.

[8] Griffiths, Phillip; Harris, Joseph. Principles of algebraic geometry. Reprint of the 1978 original. Wiley Classics Library. *John Wiley & Sons*, 1994. xiv+813 pp. ISBN: 0-471-05059-8. MR1288523 (95d:14001), Zbl 0836.14001, doi: 10.1002/9781118032527.

[9] Mayr, Ernst W.; Meyer, Albert R. The complexity of the word problems for commutative semigroups and polynomial ideals. *Adv. in Math.* **46** (1982), no. 3, 305–329. MR0683204 (84g:20099), Zbl 0506.03007, doi: 10.1016/0001-8708(82)90048-2.

[10] Milnor, J. On the Betti numbers of real varieties. *Proc. Amer. Math. Soc.* **15** (1964), 275–280. MR0161339 (28 #4547), Zbl 0123.38302, doi: 10.2307/2034050.

[11] Povero, M. Modelling Kähler manifolds and projective surfaces. Ph.D. thesis, cycle XXI. Politecnico di Torino, 2009.

[12] Salamon, Simon; Viaclovsky, Jeff. Orthogonal complex structures on domains in R^4. *Math. Ann.* **343** (2009), no. 4, 853–899. MR2471604 (2010b:53132), Zbl 1167.32017, arXiv:0704.3422, doi: 10.1007/s00208-008-0293-5.

[13] Thom, René. Sur l'homologie des variétés algébriques réelles. *Differential and combinatorial topology*, *Princeton Univ. Press, Princeton, N.J.*,1965. pp. 255–265. MR0200942 (34 #828), Zbl 0137.42503.

(John Armstrong) King's College London, Strand, London, WC2R 2LS
`john.1.armstrong@kcl.ac.uk`